Different Effects of 4-Hydroxyproline and 4-Fluoroproline on the Stability of Collagen Triple Helix

Yoshinori Nishi,[‡] Susumu Uchiyama,[‡,§] Masamitsu Doi,[∥] Yuji Nishiuchi,[⊥] Takashi Nakazawa,[#] Tadayasu Ohkubo,[‡] and Yuji Kobayashi*[,‡]

Graduate School of Pharmaceutical Sciences, Osaka University, Suita, Osaka 565-0871, Japan, Department of Materials Science, Wakayama National College of Technology, Gobo, Wakayama 644-0023, Japan, Peptide Institute Inc., Mino, Osaka 562-8686, Japan, and Department of Chemistry, Nara Women's University, Nara 630-8506, Japan

Received September 29, 2004; Revised Manuscript Received February 20, 2005

ABSTRACT: Differential scanning calorimetry (DSC) analyses of a series of collagen model peptides suggest that 4-hydroxyproline (Hyp) and 4-fluoroproline (fPro) have different effects on the stability of the collagen triple helices according to the sequence of amino acids and stereochemistry at the 4 positions of these imino acids. The thermodynamic parameters indicate that the enhanced stabilities are classified into two different types: the enthalpy term is primarily responsible for the enhanced stability of the triple helix of (Pro-Hyp^R-Gly)$_{10}$, whereas the entropy term dominates the enhanced stability of (Pro-fPro^R-Gly)$_{10}$. The difference between the molecular volumes observed in solution and intrinsic molecular volumes calculated from the crystal structure indicates the different hydration states of these peptides. (Pro-Hyp^R-Gly)$_{10}$ is highly hydrated compared to (Pro-Pro-Gly)$_{10}$, which contributes to the larger enthalpy. In contrast, the volume of (Pro-fPro^R-Gly)$_{10}$ shows a smaller degree of hydration than that of (Pro-Pro-Gly)$_{10}$. The entropic cost of forming the triple helix of the fPro-containing peptides is compensated by a decrease in an ordered structure of water molecules surrounding the peptide molecule, although the contribution of enthalpy originating from the hydration is reduced. These arguments about the different contribution of entropic and enthalpic terms were successfully applied to interpret the stability of the triple helix of (fPro^S-Pro-Gly)$_{10}$ as well.

The collagen triple helix is a unique structural motif found in proteins, with a characteristic repeat of X-Y-Gly, where X and Y are often imino acids, Pro, or 4(*R*)-Hyp (Hyp^R) (*1*). We synthesized the polytripeptides, (Pro-Pro-Gly)$_{10}$ and (Pro-Hyp^R-Gly)$_{10}$, and demonstrated that both peptides exhibit triple-helical structures at low temperature and undergo thermal transition to single random-coil states (*2*, *3*). The higher transition temperature of (Pro-Hyp^R-Gly)$_{10}$ than that of (Pro-Pro-Gly)$_{10}$ indicates that the hydroxyl group of Hyp^R residue enhances the stability of the triple-helical structure. This is consistent with the relationship between the content of Hyp^R and the thermal stability of natural collagens (*4*).

Many studies on various collagen model peptides have been carried out to explain the mechanism of this stability enhancement. An extremely ordered hydration structure formed by water bridges with the hydroxyl group of Hyp has been found in the crystal structure of (Pro-Hyp^R-Gly)$_4$-Pro-Hyp^R-Ala-(Pro-Hyp^R-Gly)$_5$ (*5*, *6*), which exhibits thermally stable triple-helical structure more than that of (Pro-Pro-Gly)$_{10}$ (*7*). However, a question arose about the significance of water bridges in stabilizing the triple helix, because the transition temperatures of both (Pro-Pro-Gly)$_{10}$ and (Pro-Hyp^R-Gly)$_{10}$ increased extensively in an anhydrous environment (*8*). To clarify this problem, Raines and co-workers studied the polytripeptides (X-Y-Gly)$_n$ containing 4-fluoroproline (fPro) and showed that the thermal stability of (Pro-fPro^R-Gly)$_{10}$ is much higher than that of (Pro-Hyp^R-Gly)$_{10}$ (*9*, *10*). Because a fluorine atom in fluoroalkanes has electron-withdrawing property but forms only a weak hydrogen bond (*11*−*13*), it was postulated that hydrogen bonding does not necessarily play an important role in stabilizing the triple-helical structure (*9*, *10*).

In contrast, some substitutions reduce the thermal stability of the triple-helical structure depending on the sequence of amino acids and stereochemistry at the 4 position of the imino acids. For example, we showed that (Pro-Hyp^S-Gly)$_{10}$ (*14*), (Hyp^S-Pro-Gly)$_{10}$ (*14*), and (Hyp^R-Pro-Gly)$_{10}$ (*15*) exist in single coils. Also, Raines and co-workers reported that (Pro-fPro^S-Gly)$_{10}$ has no tendency to form the triple helix (*16*). To explain the effect of the substitution of Pro by Hyp or fPro, Zagari and co-workers focused on the pyrrolidine ring puckering of imino acid residues (*17*). They surveyed the results of X-ray analyses on model peptides in the triple helix and found that the down form tends to take place in the X position and the up one, in Y position. It has been known that Hyp^R and fPro^R prefer the up form and Hyp^S

* To whom correspondence should be addressed. Telephone: +81-6-6879-8220. Fax: +81-6-6879-8224. E-mail: yujik@protein.osaka-u.ac.jp.

‡ Graduate School of Pharmaceutical Sciences, Osaka University.

§ Present address: Department of Biotechnology, Graduate School of Engineering, Osaka University, Suita, Osaka 565-0871, Japan.

∥ Department of Materials Science, Wakayama National College of Technology.

⊥ Peptide Institute Inc.

Department of Chemistry, Nara Women's University.

10.1021/bi047887m CCC: $30.25 © 2005 American Chemical Society
Published on Web 03/26/2005

and fPro^S prefer the down one on the basis of X-ray analyses and NMR spectroscopic and computational investigations on various proline derivatives (*17*−*24*). Thus, they proposed a rule that the replacement of Pro at the Y position with Hyp^R or fPro^R stabilizes the triple helix, whereas that of Pro at the Y position with Hyp^S or fPro^S and that of Pro at the X position with Hyp^R destabilize the triple helix. This rule involved an inconsistency that (Hyp^S-Pro-Gly)$_{10}$ does not form the triple helix (*14*). They regarded this as an exception because of the steric hindrance between the hydroxyl group of Hyp^S and the pyrrolidine ring of Pro in an adjacent chain (*17*). However, the recent result that demonstrated that (fPro^S-Pro-Gly)$_{10}$ forms a collagen triple helix (*25*, *26*) contradicts this explanation because the difference in volumes of a hydroxyl group and a fluorine atom is too small to account for the contrasting triple-helix propensity of these peptides. To rationalize all of the experimental results, it is essential to analyze the thermal stability of collagen triple helix quantitatively. We have already estimated the thermodynamic parameters of the transition from the circular dichroism (CD)[1] transition profile with the van't Hoff equation. However, as we have already pointed out in our previous paper (*25*), thermodynamic parameters obtained from the van't Hoff analysis for the triple helix to single coil embrace large uncertainties. Actually, even though the following three experiments treated the same sample, (Pro-Hyp^R-Gly)$_{10}$, the reported $\Delta H°$ values vary as 174, 220, and 134 kJ mol^{-1} in the experiments of refs *27*, *28*, and *29*, respectively. It should be noted that these parameters from DSC measurements would be problematic as well. For example, we had indicated that the thermal transition from triple helix to single coil has a strong scanning rate dependency (*30*, *31*). Although we have already reported the thermodynamic parameters estimated from the simple integration of the DSC curves in our manuscript for the short communication (*32*), the transition from the triple-helix to single-coil states should be treated as an association−dissociation system for a full discussion. Therefore, in the present study, DSC experiments were performed on the series of the model peptides with such a low scanning rate as to attain the equilibrium condition and the thermodynamic parameters are directly determined with DSC curves by taking into account the association−dissociation system between triple helix and single coil. According to the resulting thermodynamic parameters of the all model peptides, enhanced stabilities were classified into two types: enthalpy-dominant and entropy-dominant enhanced stability. Subsequently, partial molar volumes of these peptides in solution were determined by the density measurements to clarify the hydration states of the peptides in triple-helical structure. Considering these experimental results together with the calculation of intrinsic volumes using the atomic coordinates of the X-ray data, two types of enhanced stabilities were explained by the difference in the hydration states of Hyp- and fPro-containing model peptides.

[1] Abbreviations: ASA, accessible surface area; Boc, *t*-butoxycarbonyl; Bu^t, *t*-butyl; CD, circular dichroism; DIEA, *N*,*N*-diisopropylethylamine; DSC, differential scanning calorimetry; fPro, 4-fluoroproline; Fmoc, 9-fluorenylmethoxycarbonyl; HATU, *O*-7-azabenzotriazol-1-yl-1,1,3,3-tetramethyluronium hexafluorophosphate; HPLC, high-performance liquid chromatography; Hyp, 4-hydroxyproline; MALDI−TOF, matrix-assisted laser desorption/ionisation time-of-flight; PDB, Protein Data Bank; TFA, trifluoroacetic acid.

EXPERIMENTAL SECTION

Preparation of Model Peptides. (Pro-Pro-Gly)$_{10}$ and (Pro-Hyp^R-Gly)$_{10}$ were synthesized as reported previously (*33*). (Pro-fPro^R-Gly)$_{10}$, (fPro^S-Pro-Gly)$_{10}$, and (Hyp^S-Pro-Gly)$_{10}$ were synthesized using an Applied Biosystems 433A peptide synthesizer. Couplings were carried out on an Alko-PEG resin (Watanabe Chemical Industries, Ltd., 0.26 mmol g^{-1}, 0.1 mmol) using Fmoc (9-fluorenyl-methoxycarbonyl) amino acids (4.0 equiv). Fmoc-fPro^R-OH and Fmoc-fPro^S-OH were synthesized as described previously (*18*). The absolute configurations of fPro derivatives have been determined by chiral HPLC and X-ray crystallography (*18*). Fmoc-Hyp^S-(Bu^t)-OH was synthesized from Boc-Hyp^R-OH (see Scheme S1 in the Supporting Information). HATU (*O*-7-azabenzotriazol-1-yl-1,1,3,3-tetramethyluronium hexafluorophosphate) (4.0 equiv)/DIEA (*N*,*N*-diisopropylethylamine) (6.0 equiv) mediated peptide couplings. Cleavage of the peptide resin proceeded for 1 h using a TFA/water/triisopropylsilane mixture (95:2.5:2.5). The peptides were purified by high-performance liquid chromatography (HPLC) on an YMC-PACK C-18 reversed-phase column. We employed a peptide that has proven more than 97% pure as judged by HPLC. The molecular weight of each peptide was determined by MALDI−TOF mass spectrometry. Prior to a series of physicochemical analyses, a stock solution of a peptide in 100 mM acetic acid was prepared by keeping the solution at 90 °C, with an exception of that of (Pro-Pro-Gly)$_{10}$ at 60 °C, for 1 h to complete the dissociation into the monomer, followed by gradual cooling to room temperature, and equilibrated at 4 °C for 3 days so that the triple helices could be formed properly.

Analytical Ultracentrifugation. Sedimentation equilibrium analyses were performed with a Beckman Optima XL-I analytical ultracentrifuge at 10 °C using double-sector centerpieces with sapphire windows. The rotor speeds for (Pro-Pro-Gly)$_{10}$, (Pro-Hyp^R-Gly)$_{10}$, (Pro-fPro^R-Gly)$_{10}$, (fPro^S-Pro-Gly)$_{10}$, and (Hyp^S-Pro-Gly)$_{10}$ were 32 000, 30 000, 40 000, 40 000, and 45 000 rpm, respectively. Each peptide was dissolved at a concentration of 0.18−1.8 mM in 100 mM AcOH containing 100 mM NaCl. Data were collected taking the average of 8 measurements at each radial distance. Approach to equilibrium was considered to be completed when replicate scans separated by ≥6 h were indistinguishable.

Partial Specific Volume Determination. The partial specific volume of a solute ($\bar{v}$) is obtained from the concentration dependence of the density of the solution using the equation

$$\left(\frac{\partial \rho}{\partial c}\right)_{m,p} = 1 - \bar{v}\rho_0 \qquad (1)$$

where ρ and ρ_0 are the densities of the solution and the solvent, respectively (*34*). The densities of solutions of (Pro-Pro-Gly)$_{10}$, (Pro-Hyp^R-Gly)$_{10}$, (Pro-fPro^R-Gly)$_{10}$, and (fPro^S-Pro-Gly)$_{10}$ were measured using a vibrational density meter, Anton Paar DMA 5000, at 10 °C (within ±0.01 °C) and were collected by taking the average of three measurements (within $\pm 5 \times 10^{-6}$ g cm^{-3}). The concentration of a peptide in solution [c, (g cm^{-3})] was determined based on the amino acid analysis (see the Supporting Information).

Differential Scanning Calorimetry (DSC). DSC measurements were carried out on a VP-DSC calorimeter (Microcal

Inc.). The peptides were dissolved in 100 mM AcOH at a concentration of about 1.8 mM. A degassed peptide solution was loaded into a calorimeter cell and heated from 10 to 110 °C at a heating rate of 0.1 K min^{-1}. Reversibility of the transition was monitored by scanning the same sample 3 times without refilling the solution. To assess whether the thermal transition of each peptide involves only two states (a triple-helical structure and a single-coil state) or includes the presence of intermediates, the data were analyzed for both the three- and two-state models (*35*, *36*). The estimation procedures for the thermodynamic parameters considering trimer−monomer association−dissociation equilibrium and the change in the heat capacity between triple-helix (C_t) and random-coil (C_s) states, ΔC_p, are described in the Supporting Information.

Calculations of the Intrinsic Molecular Volume and the Accessible Surface Area (ASA). The intrinsic molecular volume of each model peptide in the triple-helix state was estimated using MSRoll (*37*). The atomic coordinates of the triple helix of (Pro-Pro-Gly)$_{10}$ were provided by the Protein Data Bank (PDB) code 1K6F (*38*). Those of the triple helix of (Pro-Hyp^R-Gly)$_{10}$ were given by Prof. Okuyama (Faculty of Technology, Tokyo University of Agriculture and Technology). Assuming that the triple helix has almost the same main-chain conformation for each collagen model peptide, we created the atomic coordinates of (Pro-fPro^R-Gly)$_{10}$ in the triple-helix state by substituting the hydroxyl group in (Pro-Hyp^R-Gly)$_{10}$ with a fluorine atom so that the pyrrolidine ring of all of the imino acids take the requisite ring puckering as a quantum mechanical study has suggested (*23*). The $C^\gamma-O_H$ ($C^\gamma-F$) bond length and the angles $C^\delta-C^\gamma-OH$ ($C^\delta-C^\gamma-F$) and $C^\beta-C^\gamma-OH$ ($C^\beta-C^\gamma-F$) were from ref *23* and PDB code 1CAG (*5*, *7*). The structures of the single coils of (Pro-Pro-Gly)$_{10}$, (Pro-Hyp^R-Gly)$_{10}$, and (Pro-fPro^R-Gly)$_{10}$ were obtained by energy minimization using X-PLOR (*39*). ASA of each model peptide was calculated using MSRoll (*37*), with the probe radius of water (equal to 1.4 Å). Total ASA (ASA_{total}) was assumed to be the sum of ASA_{pol}, ASA_{npol}, and $ASA_{fluorine}$, each of which corresponds to polar (amide N, carbonyl O, and hydroxyl O), nonpolar (aliphatic C and carbonyl C) (*40*), and fluorine components, respectively.

CD Spectroscopy. Measurements of CD spectra were carried out on an Aviv Model 202 spectropolarimeter. Spectra were obtained with a cell of either a 1 or 5 mm path length by averaging 8 scans from 190 to 260 nm. The peptides were dissolved in 100 mM AcOH at a concentration of 0.045 mM.

RESULTS

Sedimentation Equilibrium Experiments. The weight-averaged molecular weights at infinite dilution for (Pro-Pro-Gly)$_{10}$, (Pro-Hyp^R-Gly)$_{10}$, (Pro-fPro^R-Gly)$_{10}$, (fPro^S-Pro-Gly)$_{10}$, and (Hyp^S-Pro-Gly)$_{10}$ were determined and are listed in Table 1. They indicate that only (Hyp^S-Pro-Gly)$_{10}$ is a monomer, whereas the other peptides are trimers. Further aggregation into more than trimers was not observed for all of the peptides. The results of sedimentation equilibrium measurements are shown in Figures S1 and S2 in the Supporting Information.

Heat-Capacity Curves of Collagen Model Peptides. The heat-capacity curves at the second and third scan, without refilling the solution, completely overlapped for all peptides, indicating that these transitions are reversible processes. In the present experiment, we used a reasonably low scanning rate of 0.1 K min^{-1} to keep the system in thermal equilibrium, because the lower scanning rate of 0.05 K min^{-1} did not improve the accuracy of the measurements but adversely affected it by lowering the S/N ratio (see Figure S3 in the Supporting Information). The dependencies of heat capacity on the heating rate and peptide concentration of (Pro-Pro-Gly)$_{10}$ are shown in Figures S4 and S5 in the Supporting Information.

Table 1: Weight-Averaged Molecular Weights of Collagen Model Peptides at 10 °C

peptide	weight-averaged molecular weight (A)	molecular weight calculated from the chemical composition (B)	(A)/(B)
(Pro-Pro-Gly)$_{10}$	$(7.26 \pm 0.36) \times 10^3$	2530.8	2.87 ± 0.14
(Pro-Hyp^R-Gly)$_{10}$	$(7.48 \pm 0.37) \times 10^3$	2690.8	2.78 ± 0.14
(Pro-fPro^R-Gly)$_{10}$	$(7.94 \pm 0.40) \times 10^3$	2710.8	2.93 ± 0.15
(fPro^S-Pro-Gly)$_{10}$	$(8.31 \pm 0.42) \times 10^3$	2710.8	3.07 ± 0.15
(Hyp^S-Pro-Gly)$_{10}$[a]	$(2.17 \pm 0.11) \times 10^{3a}$	2690.8	0.81 ± 0.04[a]

[a] The partial specific volume of (Pro-Hyp^R-Gly)$_{10}$ at 10 °C is 0.612 cm^3 g^{-1}, which was applied for (Hyp^S-Pro-Gly)$_{10}$.

Miles and Bailey have reported that the biphasic transitions were observed when the scanning rate was low (below 0.25 K min^{-1}) and considered the initial peak as a rate-process endotherm (*41*). It is obvious in Figure 1 that only (Pro-Pro-Gly)$_{10}$ showed such a biphasic transition. The curve of (Pro-Pro-Gly)$_{10}$ was well-fitted to a three-state model, in which a small heat absorption peak was separately observed at a slightly lower temperature than the main peak as shown in Figure 1.

Our previous NMR study on the thermal transition of (Pro-Pro-Gly)$_{10}$ demonstrated the presence of two different triple-helical forms, i.e., H_L and H_H for a lower and a higher temperature state, respectively (*42*). Recently, we reported a H_L-H_H transition observed in an NMR study that corresponds to local conformational changes of the pyrrolidine rings of the Pro residues in the X position from an uniform down puckering to a more flexible state (*43*). Thus, the absorption at lower temperatures is associated with the transition of the triple helix from H_L to H_H and the one at higher temperatures with the transition from the triple-helix to single-coil state. These transitions were separately observed at the lower scanning rate (0.1 K min^{-1}), which were indistinguishable in the DSC measurement performed at scanning rates, 0.25−2 K min^{-1} (*30*, *31*), and were difficult to be separated because the transition temperatures are very close to each other. Our present study demonstrated also that the transition of the triple helix from H_L to H_H is a kinetically slow process. The fact that two transitions can be observed separately only with a peptide solution of high concentration and at a low scanning rate support these assignments. It is the reason that the transition from the triple-helix to single-coil state should be concentration-dependent, while the transition of the triple helix from H_L to H_H should be concentration-independent.

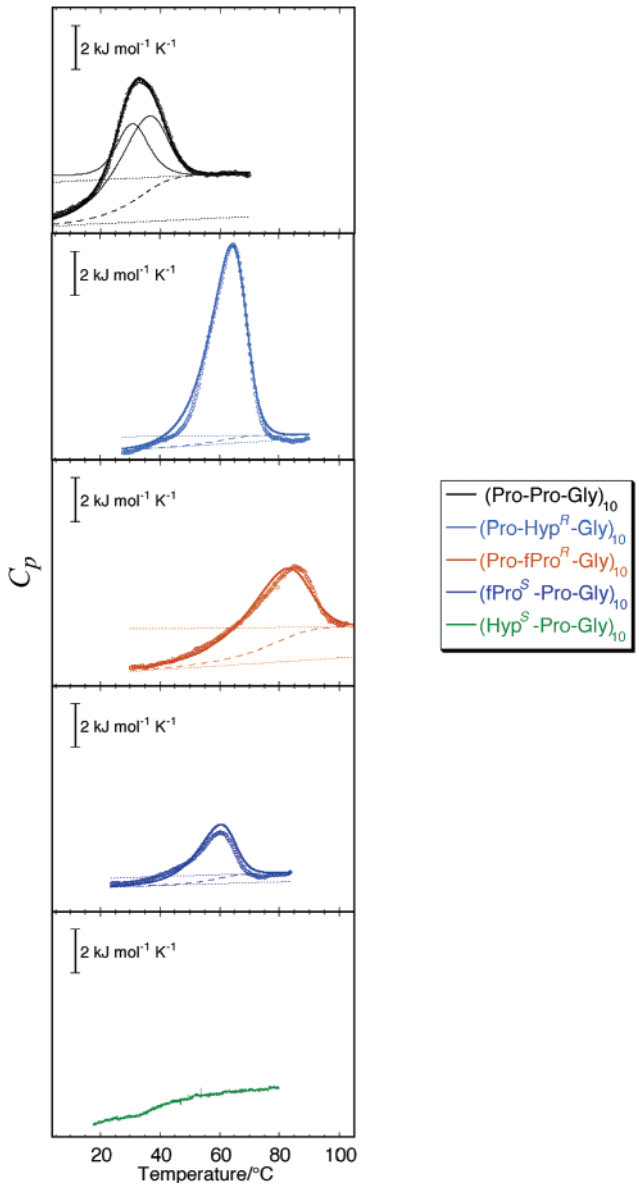

FIGURE 1: Molar heat capacity curves of (Pro-Pro-Gly)$_{10}$, (Pro-Hyp^R-Gly)$_{10}$, (Pro-fPro^R-Gly)$_{10}$, (fPro^S-Pro-Gly)$_{10}$, and (Hyp^S-Pro-Gly)$_{10}$ as a function of the temperature. For (Pro-Pro-Gly)$_{10}$, the curves deconvoluted by fitting to the three-state model are inserted.

Actually, these transitions of (Pro-Pro-Gly)$_{10}$ at such conditions are also separately observable by CD measurement, provided as Figure S6 in the Supporting Information.

In contrast to the case of (Pro-Pro-Gly)$_{10}$, the DSC curves of (Pro-Hyp^R-Gly)$_{10}$, (Pro-fPro^R-Gly)$_{10}$, and (fPro^S-Pro-Gly)$_{10}$ were fitted to the two-state model well as shown in Figure 1. Triple-helical structures of these peptides change to single-coil states without any significant intermediate. Further investigations on the transition mechanisms of these peptides are being done by NMR measurements.

The result that the heat-capacity curve of (Hyp^S-Pro-Gly)$_{10}$ showed no appreciable heat absorption (Figure 1) is consistent with the results from CD measurement and ultracentrifugation analysis by Inouye et al. that (Hyp^S-Pro-Gly)$_{10}$ does not form the triple helix at 4 °C (*14*).

Thermodynamic Parameters of the Transition. The thermodynamic parameters of the transition from the triple-helix to random-coil states, which were calculated simply by the integration of the DSC curves, have been previously reported (*32*). In this paper, the errors inherent in the preliminary thermodynamic analysis were minimized by an extensive thermodynamic analysis by treating the system as an association−dissociation equilibrium between the trimer and monomer, along with taking the difference of C_p before and after the transition into consideration. This newly developed treatment provided enthalpy change (ΔH), entropy change (ΔS), free-energy change (ΔG), and heat-capacity change (ΔC_p) associated with the transition as temperature-dependent parameters at various temperatures and made it possible for the first time to compare the thermal stabilities of each peptide at a given temperature. The resulting thermodynamic parameters of the transition for the collagen model peptides are shown in Table 2 and Figure 2. Note that transition temperature ($T_{1/2}$) is defined as the temperature where the transition is half-completed and does not correspond to the temperature where ΔG equals zero ($T°$). To compare these parameters with those of (Pro-Pro-Gly)$_{10}$, we normalized the values such as $T°\Delta S$ and ΔG at $T°_{PPG} = 71.9$ °C for $T°$ of (Pro-Pro-Gly)$_{10}$ as a reference. As illustrated in column B in Figure 2, both ΔH and $T°_{PPG}\Delta S$ of (Pro-Hyp^R-Gly)$_{10}$ were much higher than those of (Pro-Pro-Gly)$_{10}$. This shows that the increased stability of (Pro-Hyp^R-Gly)$_{10}$ results primarily from the enthalpy term. In contrast, as illustrated in columns C and D in Figure 2, both ΔH and $T°_{PPG}\Delta S$ of (Pro-fPro^R-Gly)$_{10}$ and (fPro^S-Pro-Gly)$_{10}$ were much smaller than those of (Pro-Pro-Gly)$_{10}$ and their $\Delta\Delta H$ and $T°_{PPG}\Delta\Delta S$ values were opposite in sign to those of (Pro-Hyp^R-Gly)$_{10}$, implicating that the entropic term is a dominant factor in these fPro-containing peptides.

Observed and Calculated Molar Volumes of Triple Helices. Linear relationships between concentration and density for all of the solutions of collagen model peptides forming the triple helix were obtained at 10 °C (Figure S7 in the Supporting Information). The observed partial specific volume ($\bar{v}_{obs,t}$) and observed partial molar volume ($\bar{V}_{obs,t}$) of the triple helix of each peptide at 10 °C are listed in Table 3 along with the intrinsic molecular volume of the triple helix ($V_{int,t}$) and the value of $\bar{V}_{obs,t} - V_{int,t}$. These values are those per tripeptide X-Y-Gly unit. The $\bar{V}_{obs,t}$ value of (Pro-Hyp^R-Gly)$_{10}$ is smaller than that of (Pro-Pro-Gly)$_{10}$, whereas the $\bar{V}_{obs,t}$ value of (Pro-fPro^R-Gly)$_{10}$ or (fPro^S-Pro-Gly)$_{10}$ is much larger. The $V_{int,t}$ values of these model peptides are almost the same within the range of 4.1 cm^3 mol^{-1}.

ASAs and Heat-Capacity Changes. We calculated ASAs of the collagen model peptides in their triple-helical structures (Table 3). The $ASA_{pol,t}$ value of (Pro-Hyp^R-Gly)$_{10}$ is significantly larger than that of (Pro-Pro-Gly)$_{10}$, whereas the $ASA_{npol,t}$ value of the former is considerably smaller than that of the latter. On the other hand, the value of $ASA_{npol,t}$ of (Pro-fPro^R-Gly)$_{10}$ is smaller than that of (Pro-Pro-Gly)$_{10}$, whereas the value of $ASA_{pol,t}$ of (Pro-fPro^R-Gly)$_{10}$ is almost the same as that of (Pro-Pro-Gly)$_{10}$. The values of $ASA_{fluor,t}$ of (Pro-fPro^R-Gly)$_{10}$ are considerably larger than zero because the fluorine atoms of the triple helix of (Pro-fPro^R-Gly)$_{10}$ are exposed to the solvent. The percentage of $ASA_{fluor,t}$ in the $ASA_{total,t}$ is 13% as calculated from Table 3.

Using the three-dimensional coordinates assuming the single-coil states for (Pro-Pro-Gly)$_{10}$, (Pro-Hyp^R-Gly)$_{10}$, and (Pro-fPro^R-Gly)$_{10}$, we calculated the ASA values of polar ($ASA_{pol,s}$), nonpolar ($ASA_{npol,s}$), and fluorine ($ASA_{fluor,s}$) atoms or groups in the single-coil state and the change of

Table 2: Thermodynamic Parameters of the Transition of Collagen Model Peptides

peptides	$T_{1/2}$ (°C)	$T°$ (°C)	$\Delta H(T°_{PPG})$ (kJ mol^{-1})[a]	$-T°_{PPG}\Delta S(T°_{PPG})$ (kJ mol^{-1})	$\Delta C_p(T°_{PPG})$ (J mol^{-1} K^{-1})	$\Delta G(T°_{PPG})$ (kJ mol^{-1})
(Pro-Pro-Gly)$_{10}$	31.4	71.9	108.1	−108.1	681.7	0
(Pro-Hyp^R-Gly)$_{10}$	62.2	92.3	147.1	−138.8	96.6	8.3
(Pro-fPro^R-Gly)$_{10}$	77.0	126.7	85.7	−72.0	545.7	13.7
(fPro^S-Pro-Gly)$_{10}$	54.5	116.7	65.9	−58.0	139.5	7.9

[a] $T°_{PPG}$ refers to $T° = 71.9$ °C for (Pro-Pro-Gly)$_{10}$.

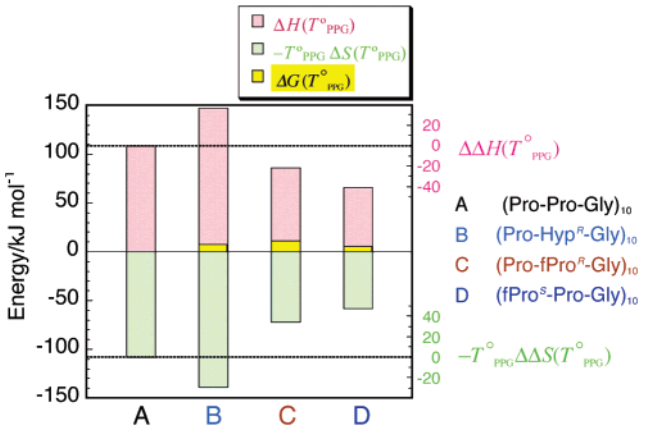

FIGURE 2: Comparison of thermodynamic parameters of the transition of collagen model peptides.

the corresponding ASA values (ΔASA$_{pol}$, ΔASA$_{npol}$, and ΔASA$_{fluor}$) associated with the conformational transition (Table 4). We assume that the heat-capacity difference of the transition of a protein can be expressed as a linear combination of ΔASA$_{pol}$, ΔASA$_{npol}$, and ΔASA$_{fluor}$ as described in the literature (*44*)

$$\Delta C_p = \Delta C°_{p,pol}\Delta\text{ASA}_{pol} + \Delta C°_{p,npol}\Delta\text{ASA}_{npol} + \Delta C°_{p,fluor}\Delta\text{ASA}_{fluor} \quad (2)$$

where $\Delta C°_{p,pol}$, $\Delta C°_{p,npol}$, and $\Delta C°_{p,fluor}$ represent the contribution of polar, nonpolar, and fluorine atoms or groups to the total ΔC_p, respectively. Equation 2 allowed us to obtain $\Delta C°_{p,pol}$ and $\Delta C°_{p,npol}$ separately by taking into account the numerical values of ΔC_p, ΔASA$_{pol}$, and ΔASA$_{npol}$ for (Pro-Pro-Gly)$_{10}$ and (Pro-Hyp^R-Gly)$_{10}$ listed in Tables 2 and 4. The results are

$$\Delta C°_{p,pol} = -0.709\ \text{J K}^{-1}\ (\text{mol Å}^2)^{-1}$$

$$\Delta C°_{p,npol} = 0.601\ \text{J K}^{-1}\ (\text{mol Å}^2)^{-1}$$

This result supports the presumption that $\Delta C°_{p,pol}$ is negative and $\Delta C°_{p,npol}$ is positive according to the general properties of proteins (*45*−*49*).

Using the resulting values, eq 2 gives

$$\Delta C°_{p,fluor} = 0.141\ \text{J K}^{-1}\ (\text{mol Å}^2)^{-1}$$

The fact that $\Delta C°_{p,fluor}$ has the same sign as that of $\Delta C°_{p,npol}$ is consistent with the fact that the fluorine atom of fPro has a hydrophobic nature.

CD Measurements. As shown in Figure 3, each CD spectrum of (Pro-Pro-Gly)$_{10}$, (Pro-Hyp^R-Gly)$_{10}$, and (Pro-fPro^R-Gly)$_{10}$ at 4 °C has a positive peak at 225 nm and a negative peak at 198 nm, which are characteristics of a triple helix. Also, their CD spectra at high temperature indicate that these model peptides exist in random coils. On the other hand, the CD spectra of (Hyp^S-Pro-Gly)$_{10}$ and (fPro^S-Pro-Gly)$_{10}$ at 4 °C shown in Figure 4A were different from others. It is obvious that (Hyp^S-Pro-Gly)$_{10}$ does not form the triple-helical structure even at low temperature. In addition, the peak of the CD pattern of (fPro^S-Pro-Gly)$_{10}$ at 225 nm is smaller than the others even though the ultracentrifugal analysis showed that it forms the triple-helical structure. In Figure 4B, there are no appreciable structural difference in the negative peaks among the model peptides detected in the single-coil state.

DISCUSSION

Resolving Intrinsic, Thermal Motion, and Hydration Contributions to the Partial Molar Volumes of Collagen Model Peptides. The observed partial molar volume of a collagen triple helix ($\bar{V}_{obs,t}$) is composed of three terms: intrinsic ($V_{int,t}$), thermal motion ($V_{therm,t}$), and hydration ($V_{hyd,t}$) volumes (*50*−*52*).

$$\bar{V}_{obs,t} = V_{int,t} + V_{therm,t} + V_{hyd,t} \quad (3)$$

Note that $V_{therm,t}$ is proportional to the total ASA value (ASA$_{total,t}$) (*50*) and that the contribution of nonpolar groups to $V_{hyd,t}$ is so small as to be negligible because of no direct interaction with solvating water molecules (*51*). These are written using numerical coefficients, *a* and *b*

$$V_{therm,t} = a\text{ASA}_{total,t} \quad (4a)$$

$$V_{hyd,t} = b\text{ASA}_{pol,t} \quad (4b)$$

Combing eqs 3, 4a, and 4b gives

$$\bar{V}_{obs,t} = V_{int,t} + a\text{ASA}_{total,t} + b\text{ASA}_{pol,t} \quad (5)$$

The Factor Stabilizing the Triple-Helical Structure for (Pro-Hyp^R-Gly)$_{10}$. Equation 5 allowed us to obtain *a* and *b* separately by taking into account the numerical values of $\bar{V}_{obs,t}$, $V_{int,t}$, ASA$_{total,t}$, and ASA$_{pol,t}$ for (Pro-Pro-Gly)$_{10}$ and (Pro-Hyp^R-Gly)$_{10}$ listed in Table 3. The results are

$$a = 0.040\ \text{cm}^3\ \text{mol}^{-1}\ \text{Å}^{-2} \qquad b = -0.12\ \text{cm}^3\ \text{mol}^{-1}\ \text{Å}^{-2}$$

Therefore, $V_{hyd,t}$ values for (Pro-Pro-Gly)$_{10}$ and (Pro-Hyp^R-Gly)$_{10}$ are −9.6 and −18.6 cm^3 mol^{-1}, respectively. To associate V_{hyd} with the degree of hydration, we rearranged eq 3 in the form

$$\bar{V}_{obs,t} = V_{int,t} + V_{therm,t} + n_{h,t}(V°_h - V°_0) \quad (6)$$

where $n_{h,t}$ is the number of water molecules involved in the hydration of a peptide in the triple-helix state (*50*−*52*), $V°_h$ is the partial molar volume of the hydration-shell water, and $V°_0$ is the molar volume of bulk water. It is known that $V°_h$

Table 3: Observed Partial Specific ($\bar{v}_{obs,t}$), Observed Partial Molar ($\bar{V}_{obs,t}$), and Intrinsic Molecular ($V_{int,t}$) Volumes and the Difference between $\bar{V}_{obs,t}$ and $V_{int,t}$ ($\bar{V}_{obs,t} - V_{int,t}$), and ASAs of the Triple-Helical Collagen Model Peptides at 10 °C

peptides	$\bar{v}_{obs,t}$ (cm^3 g^{-1})	$\bar{V}_{obs,t}$ (cm^3 mol^{-1})[a]	$V_{int,t}$ (cm^3 mol^{-1})[a]	$\bar{V}_{obs,t} - V_{int,t}$ (cm^3 mol^{-1})[a]	$ASA_{total,t}$ (Å^2)[a]	$ASA_{pol,t}$ (Å^2)[a]	$ASA_{npol,t}$ (Å^2)[a]	$ASA_{fluor,t}$ (Å^2)[a]
(Pro-Pro-Gly)$_{10}$	0.6692	169.4	157.4	12.0	539.8	79.6	460.2	0
(Pro-Hyp^R-Gly)$_{10}$	0.6120	164.7	161.5	3.2	543.7	154.6	389.1	0
(Pro-fPro^R-Gly)$_{10}$	0.7337	199.4	160.1	39.3	533.9	76.0	389.1	68.8
(fPro^S-Pro-Gly)$_{10}$	0.7331	198.7						

[a] Expressed per tripeptide unit.

Table 4: ASA Values of (Pro-Pro-Gly)$_{10}$, (Pro-Hyp^R-Gly)$_{10}$, and (Pro-fPro^R-Gly)$_{10}$ in the Triple-Helix and Single-Coil States

peptides	$ASA_{amide\ N,t}$ $ASA_{amide\ N,s}$ (Å^2)	$ASA_{carbonyl\ O,t}$ $ASA_{carbonyl\ O,s}$ (Å^2)	$ASA_{hydroxyl\ O,t}$ $ASA_{hydroxyl\ O,s}$ (Å^2)	$ASA_{aliphatic\ C,t}$ $ASA_{aliphatic\ C,s}$ (Å^2)	$ASA_{carbonyl\ C,t}$ $ASA_{carbonyl\ C,s}$ (Å^2)	$ASA_{pol,t}$ $ASA_{pol,s}$ (Å^2)	$ASA_{npol,t}$ $ASA_{npol,s}$ (Å^2)	$ASA_{fluor,t}$ $ASA_{fluor,s}$ (Å^2)	ΔASA_{pol} (Å^2)	ΔASA_{npol} (Å^2)	ΔASA_{fluor} (Å^2)
(Pro-Pro-Gly)$_{10}$	72	724	0	4477	125	796	4602	0	1581	2998	0
	588	1789	0	7453	147	2377	7600	0			
(Pro-Hyp^R-Gly)$_{10}$	68	692	785	3784	107	1545	3891	0	2092	2628	0
	508	1804	1325	6394	125	3637	6519	0			
(Pro-fPro^R-Gly)$_{10}$	68	692	0	3784	107	760	3891	688	1552	2628	474
	508	1804	0	6394	125	2312	6519	1162			

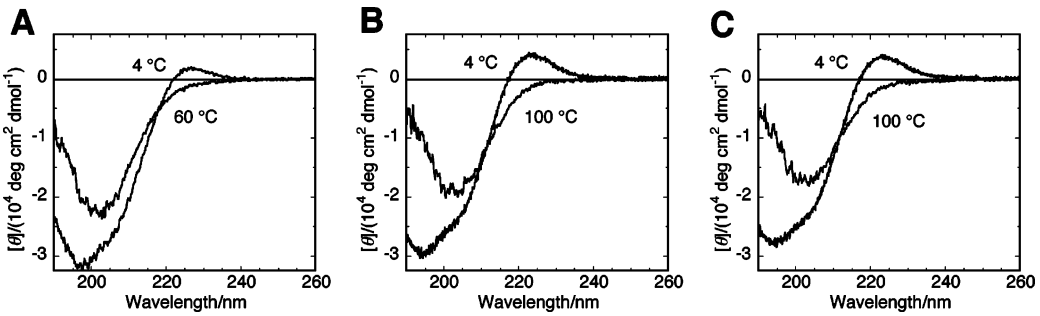

FIGURE 3: CD spectra of (A) (Pro-Pro-Gly)$_{10}$, (B) (Pro-Hyp^R-Gly)$_{10}$, and (C) (Pro-fPro^R-Gly)$_{10}$ at 4 and 100 °C with an exception of A at 4 and 60 °C. Peptide concentrations are 0.045 mM in 100 mM acetic acid.

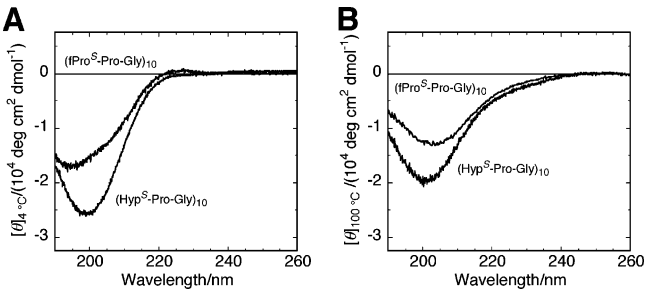

FIGURE 4: CD spectra of (Hyp^S-Pro-Gly)$_{10}$ and (fPro^S-Pro-Gly)$_{10}$ at (A) 4 °C and (B) 100 °C. Peptide concentrations are 0.045 mM in 100 mM acetic acid.

can be smaller than V_0° for a hydrophilic molecule because of the contraction of water molecules that are in contact with polar groups (*50*, *52*). Because it is possible to assume that the values of V_h° and V_0° are almost invariable among the model peptides, about twice the larger $V_{hyd,t}$ value of −18.6 cm^3 mol^{-1} for (Pro-Hyp^R-Gly)$_{10}$ than that of −9.6 cm^3 mol^{-1} for (Pro-Pro-Gly)$_{10}$ amounts to twice as many water molecules ($n_{h,t}$) being involved in the hydration of (Pro-Hyp^R-Gly)$_{10}$ as those in (Pro-Pro-Gly)$_{10}$. This is consistent with the results of the X-ray analyses of (Pro-Pro-Gly)$_{10}$ (*7*, *17*) and Hyp-containing peptides (*5*, *6*, *53*, *54*), where (Pro-Pro-Gly)$_{10}$ has only interchain water bridges connecting carbonyl groups, whereas (Pro-Hyp^R-Gly)$_{10}$ has water bridges connecting carbonyl groups with hydroxyl groups in addition to the carbonyl−carbonyl water bridges. Thus, we concluded that the larger ΔH of (Pro-Hyp^R-Gly)$_{10}$ is attributed to the increased number of hydrogen bonds including water molecules owing to the higher degree of hydration. Because ΔH of (Pro-Hyp^R-Gly)$_{10}$ is larger than that of (Pro-Pro-Gly)$_{10}$ by 39.0 kJ mol^{-1} (Table 2), we estimate 3.9 kJ mol^{-1} for the enthalpy change associated with the breaking of one hydrogen bond between a hydroxyl group and a water molecule. This value is comparable to the energy of one hydrogen bond between the hydroxyl group of a protein and a water molecule (5.2 kJ mol^{-1}) (*55*).

Hydration is one of the main factors that can reduce the entropy; an ordered hydration structure because of hydration leads to restriction of the motional freedom of the water molecules surrounding the triple helix. The stabilizing effect caused by the enthalpic term should dominate the entropic term that otherwise acts to destabilize the triple helix of (Pro-Hyp^R-Gly)$_{10}$.

The Factor Stabilizing the Triple-Helical Structure of (Pro-fPro^R-Gly)$_{10}$. Using the coefficients $a = 0.040$ cm^3 mol^{-1} Å^{-2} and $b = -0.12$ cm^3 mol^{-1} Å^{-2} in eq 5, we obtained the V_{hyd} value, 17.9 cm^3 mol^{-1}, for (Pro-fPro^R-Gly)$_{10}$, which has the opposite sign to that of (Pro-Hyp^R-Gly)$_{10}$ (−18.6 cm^3 mol^{-1}). In addition, the sign of $\Delta C^\circ_{p,fluor}$ is opposed to that of $\Delta C^\circ_{p,pol}$. These contrasting trends are probably attributed to the hydrophobic fluorine atom exposed to the solvent in fPro, opposing the hydrophilic hydroxyl group of Hyp. These results suggest that the degree of hydration of (Pro-fPro^R-Gly)$_{10}$ is much lower than that of (Pro-Hyp^R-Gly)$_{10}$ and (Pro-Pro-Gly)$_{10}$. Correspondingly, the ΔH of (Pro-fPro^R-Gly)$_{10}$ is smaller than those of (Pro-Hyp^R-Gly)$_{10}$ and (Pro-Pro-Gly)$_{10}$

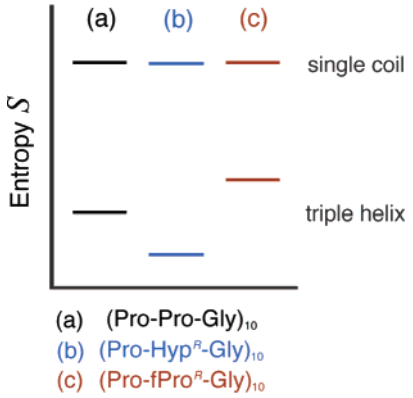

FIGURE 5: Entropy diagrams in triple-helix and single-coil states for (a) $(Pro\text{-}Pro\text{-}Gly)_{10}$, (b) $(Pro\text{-}Hyp^{R}\text{-}Gly)_{10}$, and (c) $(Pro\text{-}fPro^{R}\text{-}Gly)_{10}$.

by 61.4 and 22.4 kJ mol^{-1}, respectively (Table 2). This is consistent with the notion that a fluorine atom in fluoroalkanes is less likely to form a hydrogen bond (*9*−*11*). Assuming that the enthalpy change of breaking a hydrogen bond between a carbonyl group and a water molecule is 3.9 kJ mol^{-1} as mentioned above, only 4 of 10 carbonyl groups of $fPro^{R}$ in $(Pro\text{-}fPro^{R}\text{-}Gly)_{10}$ would participate in forming water bridges. To interpret the higher thermal stability of the triple helix of $(Pro\text{-}fPro^{R}\text{-}Gly)_{10}$, it is thus necessary to consider that the entropic term serves to compensate the smaller enthalpy change of fPro-containing peptides. The lower degree of hydration of fPro-containing peptides implies that the entropy of $(Pro\text{-}fPro^{R}\text{-}Gly)_{10}$ in the triple-helix state is higher than those of $(Pro\text{-}Hyp^{R}\text{-}Gly)_{10}$ and $(Pro\text{-}Pro\text{-}Gly)_{10}$ in the triple-helix state. Because the CD spectra shown in Figure 3 indicate that neither of these model peptides appears to form any secondary structure in high temperature, we can reasonably consider that the conformational entropies of $(Pro\text{-}Pro\text{-}Gly)_{10}$, $(Pro\text{-}Hyp^{R}\text{-}Gly)_{10}$, and $(Pro\text{-}fPro^{R}\text{-}Gly)_{10}$ in the single-coil states are the same. Finally, by assuming that the degree of hydration in the single-coil state is indistinguishable for these three collagen model peptides, total entropies of these three collagen model peptides in the single-coil state are similar to each other. The entropies of the model peptides are compared in a diagram shown in Figure 5. Because we have designated the entropy difference between the triple-helix and single-coil states as ΔS, $(Pro\text{-}fPro^{R}\text{-}Gly)_{10}$ has a smaller ΔS than those of $(Pro\text{-}Hyp^{R}\text{-}Gly)_{10}$ and $(Pro\text{-}Pro\text{-}Gly)_{10}$, as illustrated in Figure 5.

A recent host−guest experiment has shown that the triple helix of $Ac\text{-}Gly\text{-}(Pro\text{-}Hyp^{R}\text{-}Gly)_{3}\text{-}Pro\text{-}fPro^{R}\text{-}Gly\text{-}(Pro\text{-}Hyp^{R}\text{-}Gly)_{4}\text{-}Gly\text{-}NH_2$ is somewhat less stable than the corresponding one that involves the simple $Pro\text{-}Hyp^{R}\text{-}Gly$ repeats, contradicting the expected preference of $Pro\text{-}fPro^{R}\text{-}Gly$ to a polyproline-II-like structure (*56*). Note that this result could also be understood in terms of distinct contributions of enthalpy and entropy terms to stabilize the triple helix containing Hyp and fPro, respectively. That is, $Pro\text{-}fPro^{R}$ in the context of $Ac\text{-}Gly\text{-}(Pro\text{-}Hyp^{R}\text{-}Gly)_{3}\text{-}X\text{-}Y\text{-}Gly\text{-}(Pro\text{-}Hyp^{R}\text{-}Gly)_{4}\text{-}Gly\text{-}NH_2$ can interrupt the water network, leading to a slight loss of hydration enthalpy relative to $Ac\text{-}Gly\text{-}(Pro\text{-}Hyp^{R}\text{-}Gly)_{8}\text{-}Gly\text{-}NH_2$. The entropic gain attributable to one fPro residue embedded in the midst of a long peptide chain may not be sufficient to counteract the loss of such hydration enthalpy.

The Factor Stabilizing the Triple-Helical Structure of $(fPro^{S}\text{-}Pro\text{-}Gly)_{10}$. Because the $\bar{V}_{obs,t}$ value of $(fPro^{S}\text{-}Pro\text{-}Gly)_{10}$ is almost identical to that of $(Pro\text{-}fPro^{R}\text{-}Gly)_{10}$, the stabilizing mechanism of the triple helix for $(Pro\text{-}fPro^{R}\text{-}Gly)_{10}$ and $(fPro^{S}\text{-}Pro\text{-}Gly)_{10}$ will be similar to each other. However, ΔH, ΔS, and ΔC_p values of $(fPro^{S}\text{-}Pro\text{-}Gly)_{10}$ are significantly smaller than those of $(Pro\text{-}fPro^{R}\text{-}Gly)_{10}$. In the CD spectra of $(Pro\text{-}fPro^{R}\text{-}Gly)_{10}$ and $(fPro^{S}\text{-}Pro\text{-}Gly)_{10}$ at 4 °C, there appears a considerable difference in the molar ellipticity in the region 195−230 nm, indicating that their triple helices are not quite the same (Figures 3C and 4A). The lower molar ellipticity of $(fPro^{S}\text{-}Pro\text{-}Gly)_{10}$ could possibly be attributed to the looser fold than the ordinary triple-helical structure of $(Pro\text{-}fPro^{R}\text{-}Gly)_{10}$ with respect to the Rich−Crick hydrogen bonds between the Gly NH proton and the carbonyl group of imino acids in the X position of the adjacent chain (*57*). It is very likely that the smaller ΔH of $(fPro^{S}\text{-}Pro\text{-}Gly)_{10}$ than $(Pro\text{-}fPro^{R}\text{-}Gly)_{10}$ is attributable to the imperfect pattern for Rich−Crick hydrogen bonds, because breaking Rich−Crick hydrogen bonds is needed to dissociate the triple helix. The smaller ΔS results from a higher degree of freedom in the triple-helix state.

Opposite Propensities of $(Hyp^{S}\text{-}Pro\text{-}Gly)_{10}$ *and* $(fPro^{S}\text{-}Pro\text{-}Gly)_{10}$ *for the Triple Helix*. It is evident, from the molecular weights determined by sedimentation equilibrium experiments at 10 °C, that $(Hyp^{S}\text{-}Pro\text{-}Gly)_{10}$ does not form the triple helix but that $(fPro^{S}\text{-}Pro\text{-}Gly)_{10}$ does (Table 1). The possibility of $(Hyp^{S}\text{-}Pro\text{-}Gly)_{10}$ undergoing an even less considerable structural transition is excluded by the results of DSC measurements (Figure 1). The opposite propensities of these peptides for the triple-helix formation are also implicated by the presence and absence of positive absorption at 220−230 nm in the CD spectra measured at 4 °C (Figure 4A). There is no other reasonable explanation why $(Hyp^{S}\text{-}Pro\text{-}Gly)_{10}$ does not form the triple helix than the possibility of steric hindrance proposed by Zagari and co-workers (*17*). However, as we mentioned above, it should be discussed totally from both aspects of structural and thermodynamic views.

The structure determination of $(fPro^{S}\text{-}Pro\text{-}Gly)_{10}$ by either a theoretical or an experimental method, which is in progress, will provide us with the manner of stabilization. Furthermore, it is unlikely that Hyp^{S} is capable of replacing $fPro^{S}$ without affecting the interaction with water molecules, even though the molecular geometries of Hyp^{S} and $fPro^{S}$ are similar (*23*). If hydration of Hyp^{S} serves to favorably stabilize the triple helix, there is a possibility that $(Hyp^{S}\text{-}Pro\text{-}Gly)_{n}$ forms the triple helix as its degree of polymerization (n) increases to much higher than 10, because the hydroxyl group of Hyp^{S} should not appreciably differ from the fluorine atom of $fPro^{S}$ as far as the molecular volume and geometrical parameters of the pyrrolidine ring are concerned (*23*). Expecting to obtain thermodynamic parameters associated with the possible monomer−trimer transition, we are now synthesizing $(Hyp^{S}\text{-}Pro\text{-}Gly)_{n}$ ($n > 10$) that may form a triple helix above 4 °C as well.

CONCLUSION

Contributions of the hydroxyl group of Hyp and the fluorine atom of fPro at the Y position of $(X\text{-}Y\text{-}Gly)_{n}$ have been discussed based on the same stabilizing mechanism.

Our present thermodynamic analyses clearly explain enhanced thermal stabilities of Hyp- and fPro-containing collagen model peptides. This conclusion is based on direct thermodynamic measurements. Furthermore, a plausible explanation for favorable enthalpy and entropy terms is presented based on the comparison of molecular volumes observed in solution with intrinsic ones from the crystal structure. Further, precise analysis, with regard to structures of the collagen model peptides in the random-coil state as well as in the triple-helix state, should be carried out for complete understanding of the stabilizing mechanism of collagen triple helix. Recently, various kinds of interesting collagen peptides in addition to these mentioned here have been synthesized and characterized, including peptides of which X and Y positions are substituted simultaneously (*58*−*60*). Thermodynamic analyses on such peptides from the aspect in this context should be promising to shed light on thermal stability of a naturally occurring collagen molecule.

ACKNOWLEDGMENT

We thank Dr. S. Kubo and Dr. H. Nishio (Peptide Institute Inc.) for the characterization of the model peptides with mass spectrometry and Ms. Y. Yagi (Institute for Protein Research, Osaka University) for the precise amino acid analyses for concentration determination of peptide solution. We thank Dr. T. Tomiyama (Department of Chemistry, Graduate School of Science, Nagoya University) and Dr. K. Fukada (Faculty of Agriculture, Kagawa University) for technical support of density measurement. We also thank Mr. S. Nakamura (Graduate School of Pharmaceutical Sciences, Osaka University) for calculating molecular volumes and ASAs of model peptides.

SUPPORTING INFORMATION AVAILABLE

Synthetic scheme for the preparation of Fmoc-Hyp^{S}(Bu^{t})-OH, the mathematical derivations of DSC analysis, the results of sedimentation equilibrium experiments, the DSC curves of the collagen model peptides with various heating rate, and the heating rate dependencies of the transition temperature. This material is available free of charge via the Internet at http://pubs.acs.org.

REFERENCES

1. Baum, J., and Brodsky, B. (2000) Folding of the collagen triple-helix and its naturally occurring mutants, in *Mechanisms of Protein Folding* (Pain, R. H., Ed.) 2nd ed., pp 330−351, Oxford University Press, Oxford, U.K.
2. Kobayashi, Y., Sakai, R., Kakiuchi, K., and Isemura, T. (1970) Physicochemical analysis of (Pro-Pro-Gly)$_n$ with defined molecular weight-temperature dependence of molecular weight in aqueous solution, *Biopolymers 9*, 415−425.
3. Sakakibara, S., Inouye, K., Shudo, K., Kishida, Y., Kobayashi, Y., and Prockop, D. J. (1973) Synthesis of (Pro-Hyp-Gly)$_n$ of defined molecular weights. Evidence for the stabilization of collagen triple helix by hydroxyproline, *Biochim. Biophys. Acta 303*, 198−202.
4. Burjanadze, T. V. (1992) Thermodynamic substantiation of water-bridged collagen structure, *Biopolymers 32*, 941−949.
5. Bella, J., Eaton, M., Brodsky, B., and Berman, H. M. (1994) Crystal and molecular structure of a collagen-like peptide at 1.9 Å resolution, *Science 266*, 75−81.
6. Bella, J., Brodsky, B., and Berman, H. M. (1995) Hydration structure of a collagen peptide, *Structure 3*, 893−906.
7. Kramer, R. Z., Vitagliano, L., Bella, J., Berisio, R., Mazzarella, L., Brodsky, B., Zagari, A., and Berman, H. M. (1998) X-ray crystallographic determination of a collagen-like peptide with the repeating sequence (Pro-Pro-Gly), *J. Mol. Biol. 280*, 623−638.
8. Engel, J., Chen, H., Prockop, D. J., and Klump, H. (1977) The triple helix in equilibrium with coil conversion of collagen-like polytripeptides in aqueous and nonaqueous solvents. Comparison of the thermodynamic parameters and the binding of water to (L-Pro-L-Pro-Gly)$_n$ and (L-Pro-L-Hyp-Gly)$_n$, *Biopolymers 16*, 601−622.
9. Holmgren, S. K., Taylor, K. M., Bretscher, L. E., and Raines, R. T. (1998) Code for collagen's stability deciphered, *Nature 392*, 666−667.
10. Holmgren, S. K., Bretscher, L. E., Taylor, K. M., and Raines, R. T. (1999) A hyperstable collagen mimic, *Chem. Biol. 6*, 63−70.
11. Howard, J. A. K., Hoy, V. J., O'Hagan, D., and Smith, G. T. (1996) How good is fluorine as a hydrogen bond acceptor? *Tetrahedron 52*, 12613−12622.
12. Dunitz, J. D., and Taylor, R. (1997) Organic fluorine hardly ever accepts hydrogen bonds, *Eur. J. Chem. 3*, 89−98.
13. Hiyama, T., Kanie, K., Kusumoto, T., Morizawa, Y., and Shimizu, M. (2000) Properties of fluoroorganic compounds, in *Organofluorine Compounds: Chemistry and Applications* (Hiyama, T., Ed.), pp 10−12, Springer, Berlin, Germany.
14. Inouye, K., Sakakibara, S., and Prockop, D. J. (1976) Effects of the stereo-configuration of the hydroxyl group in 4-hydroxyproline on the triple-helical structures formed by homogeneous peptides resembling collagen, *Biochim. Biophys. Acta 420*, 133−141.
15. Inouye, K., Kobayashi, Y., Kyogoku, Y., Kishida, Y., Sakakibara, S., and Prockop D. J. (1982) Synthesis and physical properties of (hydroxyproline-proline-glycine)$_{10}$: Hydroxyproline in the *X*-position decreases the melting temperature of the collagen triple helix, *Arch. Biochem. Biophys. 219*, 198−203.
16. Bretscher, L. E., Jenkins, C. L., Taylor, K. M., and Raines, R. T. (2001) Conformational stability of collagen relies on a stereoelectronic effect, *J. Am. Chem. Soc. 123*, 777−778.
17. Vitagliano, L., Berisio, R., Mazzarella, L., and Zagari, A. (2001) Structural bases of collagen stabilization induced by proline hydroxylation, *Biopolymers 58*, 459−464.
18. Doi, M., Nishi, Y., Kiritoshi, N., Iwata, T., Nago, M., Nakano, H., Uchiyama, S., Nakazawa, T., Wakamiya, T., and Kobayashi, Y. (2002) Simple and efficient syntheses of Boc- and Fmoc-protected 4(*R*)- and 4(*S*)-fluoroproline solely from 4(*R*)-hydroxyproline, *Tetrahedron 58*, 8453−8459.
19. Gerig, J. T., and McLeod, R. S. (1973) Conformations of *cis*- and *trans*-4-fluoro-L-proline in aqueous solution, *J. Am. Chem. Soc. 95*, 5725−5729.
20. Shamala, M., Row, T. N. G., and Venkatesan, K. (1976) Crystal and molecular structure of *allo*-4-hydroxy-L-proline dehydrate, *Acta Crystallogr., Sect. B 32*, 3267−3270.
21. Panasik, N., Jr., Eberhardt, E. S., Edison, A. S., Powell, D. R., and Raines, R. T. (1994) Inductive effects on the structure of proline residues, *Int. J. Pept. Protein Res. 44*, 262−269.
22. Vitagliano, L., Berisio, R., Mastrangelo, A., Mazzarella, L., and Zagari, A. (2001) Preferred proline puckerings in *cis* and *trans* peptide groups: Implications for collagen stability, *Protein Sci. 10*, 2627−2632.
23. Improta, R., Benzi, C., and Barone, V. (2001) Understanding the role of stereoelectronic effects in determining collagen stability. 1. A quantum mechanical study of proline, hydroxyproline, and fluoroproline dipeptide analogues in aqueous solution, *J. Am. Chem. Soc. 123*, 12568−12577.
24. DeRider, M. L., Wilkens, S. T., Waddell, M. J., Bretscher, L. E., Weinhold, F., Raines, R. T., and Markley, J. L. (2002) Collagen stability: Insights from NMR spectroscopic and hybrid density functional computational investigations of the effect of electronegative substituents on prolyl ring conformations, *J. Am. Chem. Soc. 124*, 2497−2505.
25. Doi, M., Nishi, Y., Uchiyama, S., Nishiuchi, Y., Nakazawa, T., Ohkubo, T., and Kobayashi, Y. (2003) Characterization of collagen model peptides containing 4-fluoroproline; (4(*S*)-fluoroproline-Pro-Gly)$_{10}$ forms a triple helix, but (4(*R*)-fluoroproline-Pro-Gly)$_{10}$ does not, *J. Am. Chem. Soc. 125*, 9922−9923.
26. Hodges, J. A., and Raines, R. T. (2003) Stereoelectronic effects on collagen stability: The dichotomy of 4-fluoroproline diastereomers, *J. Am. Chem. Soc. 125*, 9262−9263.
27. Long, C. G., Braswell, E., Zhu, D., Apigo, J., Baum, J., and Brodsky, B. (1993) Characterization of collagen-like peptides containing interruptions in the repeating Gly-X-Y sequence, *Biochemistry 32*, 11688−11695.

28. Venugopal, M. G., Ramshaw, J. A. M., Braswell, E., Zhu, D., and Brodsky, B. (1994) Electrostatic interactions in collagen-like triple-helical peptides, *Biochemistry 33*, 7948−7956.
29. Engel, J., and Bächinger, H. P. (2000) Cooperative equilibrium transitions coupled with a slow annealing step explain the sharpness and hysteresis of collagen folding, *Matrix Biol. 19*, 235−244.
30. Kajiyama, K., Tomiyama, T., Uchiyama, S., and Kobayashi, Y. (1995) Phase transitions of sequenced polytripeptides observed by microcalorimetry, *Chem. Phys. Lett. 247*, 299−303.
31. Uchiyama, S., Kai, T., Kajiyama, K., Kobayashi, Y., and Tomiyama, T. (1997) Measurement of thermodynamic quantities in the heating-rate dependent thermal transitions of sequenced polytripeptides, *Chem. Phys. Lett. 281*, 92−96.
32. Nishi, Y., Doi, M., Uchiyama, S., Nishiuchi, Y., Nakazawa, T., Ohkubo, T., and Kobayashi, Y. (2003) Stabilization mechanism of triple helical structure of collagen molecules, *Lett. Pept. Sci. 10*, 533−537.
33. Sakakibara, S., Kishida, Y., Kikuchi, Y., Sakai, R., and Kakiuchi, K. (1968) Synthesis of poly-(L-prolyl-L-prolylglycyl) of defined molecular weights, *Bull. Chem. Soc. Jpn. 41*, 1273.
34. Kupke, D. W. (1973) Density and volume change measurements, in *Physical Principles and Techniques of Protein Chemistry, Part C* (Leach, S. J., Ed.), pp 1−75, Academic Press, New York.
35. Thompson, K. S., Vinson, C. R., and Freire, E. (1993) Thermodynamic characterization of the structural stability of the coiled-coil region of the bZIP transcription factor GCN4, *Biochemistry 32*, 5491−5496.
36. Johnson, C. R., Morin, P. E., Arrowsmith, C. H., and Freire, E. (1995) Thermodynamic analysis of the structural stability of the tetrameric oligomerization domain of p53 tumor suppressor, *Biochemistry 34*, 5309−5316.
37. Connoly, M. L. (1983) Analytical molecular surface calculation, *J. Appl. Crystallogr. 16*, 548−558.
38. Berisio, R., Vitagliano, L., Mazzarella, L., and Zagari, A. (2002) Crystal structure of the collagen triple helix model $[(Pro\text{-}Pro\text{-}Gly)_{10}]_3$, *Protein Sci. 11*, 262−270.
39. Brünger, A. T. (1992) *X-PLOR Version 3.1: A System for X-ray Crystallography and NMR*, Yale University, New Haven, CT.
40. Richards, F. M. (1977) Areas, volumes, packing, and protein structure, *Annu. Rev. Biophys. Bioeng. 6*, 151−176.
41. Miles, C. A., and Bailey, A. J. (2004) Studies of the collagen-like peptide $(Pro\text{-}Pro\text{-}Gly)_{10}$ confirm that the shape and position of the type I collagen denaturation endotherm is governed by the rate of helix unfolding, *J. Mol. Biol. 337*, 917−931.
42. Kai, T., Uchiyama, S., Yoshida, T., Kobayashi, Y., Kajiyama, K., and Tomiyama, T. (1997) NMR observation of two states of triple helix in the thermal transition of $(Pro\text{-}Pro\text{-}Gly)_{10}$, *Chem. Phys. Lett. 281*, 86−91.
43. Kai, T., Uchiyama, S., Nishi, Y., Kobayashi, Y., and Tomiyama, T. (2004) Two states of the triple helix in the thermal transition of the collagen model peptide $(Pro\text{-}Pro\text{-}Gly)_{10}$, *J. Biomol. Struct. Dyn. 22*, 51−58.
44. Freire, E. (1994) Statistical thermodynamic analysis of differential scanning calorimetry data: Structural deconvolution of heat capacity function of proteins, *Methods Enzymol. 240*, 502−530.
45. Makhatadze, G. I., and Privalov, P. L. (1990) Heat capacity of proteins. I. Partial molar heat capacity of individual amino acid residues in aqueous solution: Hydration effect, *J. Mol. Biol. 213*, 375−384.
46. Privalov, P. L., and Makhatadze, G. I. (1990) Heat capacity of proteins. II. Partial molar heat capacity of the unfolded polypeptide chain of proteins: Protein unfolding effects, *J. Mol. Biol. 213*, 385−391.
47. Murphy, K. P., and Gill, S. J. (1990) Group additivity thermodynamics for dissolution of solid cyclic dipeptides into water, *Thermochim. Acta 172*, 11−20.
48. Murphy, K. P., and Gill, S. J. (1991) Solid model compounds and the thermodynamics of protein unfolding, *J. Mol. Biol. 222*, 699−709.
49. Murphy, K. P., and Freire, E. (1992) Thermodynamics of structural stability and cooperative folding behavior in proteins, *Adv. Protein Chem. 43*, 313−361.
50. Chalikian, T. V., Totrov, M., Abagyan, R., and Breslauer, K. J. (1996) The hydration of globular proteins as derived from volume and compressibility measurements: Cross correlating thermodynamic and structural data, *J. Mol. Biol. 260*, 588−603.
51. Kharakoz, D. P. (1992) Partial molar volumes of molecules or arbitrary shape and the effect of hydrogen bonding with water, *J. Solution Chem. 21*, 569−595.
52. Chalikian, T. V., and Filfil, R. (2003) How large are the volume changes accompanying protein transitions and binding? *Biophys. Chem. 104*, 489−499.
53. Kramer, R. Z., Venugopal, M. G., Bella, J., Mayville, P., Brodsky, B., and Berman, H. M. (2000) Staggered molecular packing in crystals of a collagen-like peptide with a single charged pair, *J. Mol. Biol. 301*, 1191−1205.
54. Berisio, R., Vitagliano, L., Mazzarella, L., and Zagari, A. (2001) Crystal structure of a collagen-like polypeptide with repeating sequence Pro-Hyp-Gly at 1.4 Å resolution: Implications for collagen hydration, *Biopolymers 56*, 8−13.
55. Takano, K., Yamagata, Y., Funahashi, J., Hioki, Y., Kuramitsu, S., and Yutani, K. (1999) Contribution of intra- and intermolecular hydrogen bonds to the conformational stability of human lysozyme, *Biochemistry 38*, 12698−12708.
56. Persikov, A. V., Ramshaw, J. A. M., Kirkpatrick, A., and Brodsky, B. (2003) Triple-helix propensity of hydroxyproline and fluoroproline: Comparison of host−guest and repeating tripeptide collagen models, *J. Am. Chem. Soc. 125*, 12500−12501.
57. Rich, A., and Crick, F. H. C. (1961) The molecular structure of collagen, *J. Mol. Biol. 3*, 483−506.
58. Barth, D., Milbradt, A. G., Renner, C., and Moroder, L. (2004) A (4*R*)- or a (4*S*)-fluoroproline residue in position Xaa of the (Xaa-Yaa-Gly) collagen repeat severely affects triple-helix formation, *ChemBioChem 5*, 79−86.
59. Mizuno, K., Hayashi, T., Peyton, D. H., and Bächinger, H. P. (2004) Hydroxylation-induced stabilization of the collagen triple helix: Acetyl-(glycyl-4(*R*)-hydroxyprolyl-4(*R*)-hydroxyprolyl)$_{10}$-NH_2 forms a highly stable triple helix, *J. Biol. Chem. 279*, 38072−38078.
60. Berisio, R., Granata, V., Vitagliano, L., and Zagari, A. (2004) Imino acids and collagen triple helix stability: Characterization of collagen-like polypeptides containing Hyp-Hyp-Gly sequence repeats, *J. Am. Chem. Soc. 126*, 11402−11403.

BI047887M